24th INTERNATIONAL CONGRESS ON SOUND AND VIBRATION
23–27 July 2017, London

ICSV24
23-27JULY 2017
LONDON CALLING

EXPERIMENTAL OBSERVATIONS OF FLOW-ACOUSTIC FEEDBACK PHENOMENA IN DUCTS

Jean-Michel Ville, Nicolas Papaxanthos, Emmanuel Perrey-Debain

and Solène Moreau

Laboratoire Roberval UMR CNRS 7337
Sorbonne Universités, Université de Technologie de Compiègne
CS 60319, 60203 Compiègne, France
email: emmanuel.perrey-debain@utc.fr

Saad Bennouna

Valeo Thermal Systems
8 rue Louis Lormand, 78320 La Verrière, France

Excitation of flow-acoustic feedback mechanisms by turbulent internal flows has long been recognized, but the industry continues to be plagued by its undesirable consequences, manifested in severe vibration and noise problems in a wide range of industrial applications.
In this work, instabilities of separated shear flows and their coupling mechanisms with sound waves are experimentally observed. Two scenarios are investigated: the first one concerns that of a ducted tandem diaphragm in which the fluid-dynamic mechanism is caused by flow impingement on the second diaphragm, the second one concerns that a fluid-resonant mechanism caused by the excitation of quasi-trapped modes that exists in the vicinity of a flap inserted in a duct. In both cases, flow-acoustic feedback phenomena are identified via the measurement of the sound power level carried by upstream and downstream acoustic modes in the duct using an acoustic 2N-port model. Comparisons with computed results using Lighthill's analogy are also shown and discussed.

Keywords: flow-acoustic feedback, duct acoustics

1. Introduction

To obtain a satisfactory indoor environment, the acoustical design of a ventilation systems (HVAC) is as important as its thermal design becoming even more significant since the development of the electrical and hybrid electric vehicles. The HVAC noise is in part caused by the turbulent low Mach number flow interactions with multiple in-duct discontinuities (flaps, filter, heat exchanger, bends…) located in a compact housing duct. To predict the Sound Power Level (SWL) spectra of these aero-acoustic sources usually the Nelson-Morfey's theory [1] which assumes a dipole source distribution resulting of the drag fluctuating forces arising from the turbulent flow in the vicinity of the element was used leading to typical broadband spectra. However, several experimental works have pointed out amplifications and whistling effects in a car HVAC [2,3] which are shown to be produced by fluid-acoustic interaction. Indeed, basically, there are three different mechanisms which generate upstream feedback of disturbance [4]: structural vibrations, fluid-resonant mechanism triggered when the frequency of vorticity shedding becomes close to that of an acoustic resonator and the fluid-dynamic mechanism caused by flow impingement on a downstream object. The aim of this paper is to

point out experimentally that the coupling between flow instability and an upstream feedback can be responsible for noise amplifications. Two scenarios representing the association of HVAC elements are investigated: a butterfly flap and and two diaphragms in tandem.

2. The 2N-ports method procedure and hardware

To characterize the aero-acoustic source, experiments are performed assuming that each tested element is located in a hard wall straight duct H=0.1m high and W=0.2m width with rectangular cross section.

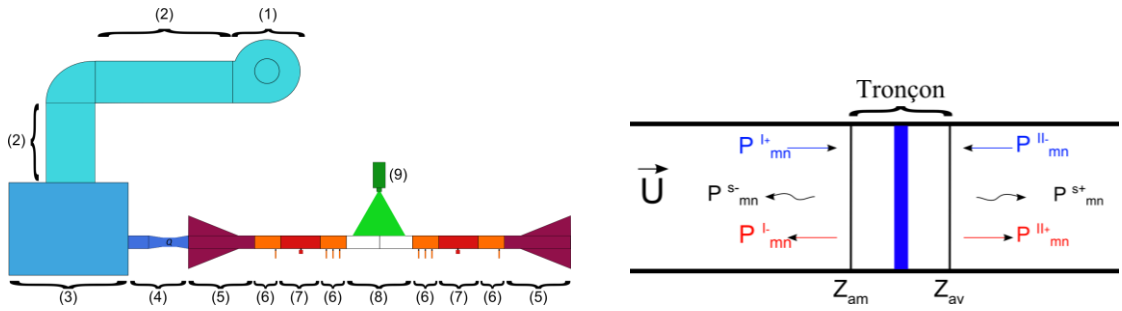

Figure 1: Duct flow facility hardware and the 2N-ports representation (acoustic duct mode indices m and n corresponds to transversal coordinates and U is the mean velocity of the flow).

The radiated acoustic waves propagating downstream and upstream of the test section are expressed as duct acoustic mode amplitudes P^{so} and are related to the incoming pressures P^{en} and to the acoustic pressure P^{s} which corresponds to the possible existence of an acoustic source located in the test section. This is conveniently described as the 2N-ports formulation [5]:

$$P^{so} = \boldsymbol{S}\, P^{en} + P^{s}, \tag{1}$$

where $\boldsymbol{S}$ is the scattering matrix of the test section. The aim of the experiment is to measure the scattering matrix and the source vector P^{s} up to 3500Hz where N=8 duct modes are cut-on. The duct flow facility and the experimental procedure (Fig. 1) are detailed in [5]. The two diaphragms in tandem and the flap are shown in Fig. 2. Measurements are conducted for mean flow velocities from 1.7 up to 7m/s, three distances L =0.06, 0.13 and 0.21m between the two diaphragms. The flap is a square edge t=0.004m thick plate and its length is h=H (0.1m) with therefore a ratio $h/t = 25$. The opening angle α is varying from nearly closed case α=15° up to horizontal position α=90°. The effective length along the duct axis of the test section occupied by the flap is given by $L = h \sin \alpha$.

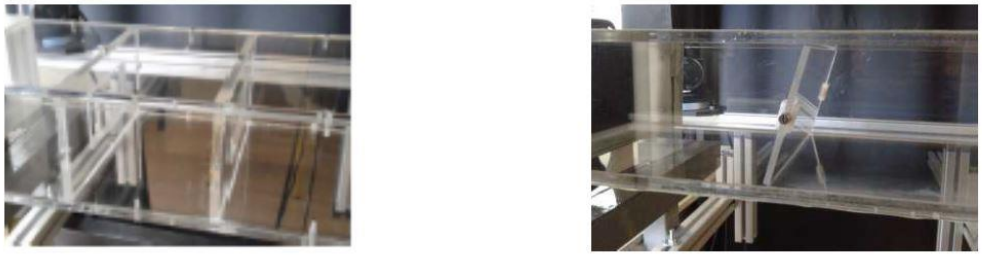

Figure 2: The two diaphragms in tandem and the flap in the test section.

3. Diaphragms in tandem

The total SWL radiated by the aero-acoustic source for three values for L are compared with the SWL of a single diaphragm for a mean flow velocity U=6.95m/s (Fig. 3).

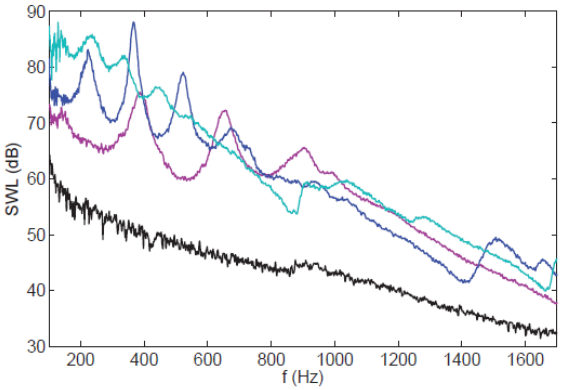

Figure 3: SWL for a single diaphragm (black) and a tandem with L=0.06m (pink), 0.13m (blue) and L=0.21m (green).

With the tandem the broadband noise is increased by more than 20dB with the presence of peaks at low frequencies. These tones are the result of a feedback effect produced by the vortices impingement on the second diaphragm causing acoustic waves propagating upstream and triggering a new set of vortices. They are known as the Rossiter's frequencies [6] which depend upon U and L as given by:

$$f_n = \frac{n-\varepsilon}{L\left(\frac{1}{U_c}+\frac{1}{c_0}\right)} \quad , \tag{2}$$

where n is the number of vortices located between both diaphragms and ε is an empirical constant associated to the delay between the flow impact on the downstream obstacle and the start of the acoustic wave propagating upstream at c_0 is the speed of sound. The convection velocity U_c of the vortices is estimated via numerical simulations (see Fig. 4 left).

Comparisons with computed results using Lighthill's analogy are now discussed. The flow simulation is carried out on 160 CPUs with the finite volume commercial software Star-CCM+. Fig.4 (left) illustrates the instantaneous incompressible-flow pressure. The acoustic field generated by the turbulent flow is obtained by solving the integral form of Lighthill's equation [7] from data calculated with the incompressible-flow LES and appropriate radiation conditions are imposed at both ends of the duct. Fig. 4 (right) shows the calculated as well as the measured total sound power radiated downstream the obstacle for a tandem diaphragm with L= 0.13m. Numerical results match fairly well with the experimental data except around the Rossiter's frequencies. This indicates that these effects are not from pure acoustic resonance as this would have been identified by our numerical prediction and such feedback mechanisms cannot be captured with acoustic analogies based on incompressible-flow solvers.

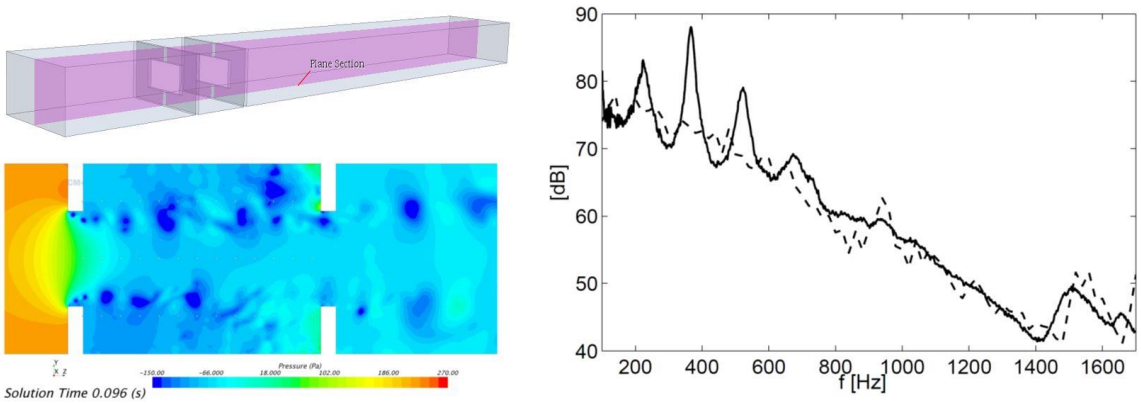

Figure 4: Left: Computational domain and instantaneous incompressible-flow pressure calculated with LES Star-CCM+. Right: SWL for a tandem diaphragm with L= 0.13m, straight line: experiments, dashed: computed.

4. Butterfly flap

The total upstream and downstream SWL radiated by the flap for three mean flow velocities are plotted in Fig. 5 pointing out that around 2500Hz the SWL is higher than the SWL for higher flow velocities which is not expected by the Nelson's theory.

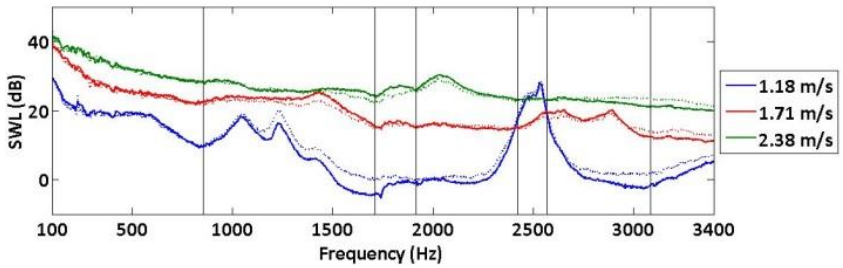

Figure 5: SWL radiated downstream (-) and upstream (⋯) of the flap for α = 30°.

The analysis of this result is based on an experiment conducted in the 60's by Parker [8] who showed that high SPL at discrete frequencies can be the result of a coincidence between the frequency of the vortex shedding produced by the interaction of the flow with an horizontal flat plate located on the center line of a duct and the resonance frequencies of the acoustic modes of the cavity around the plate, well known today as Parker's modes. In the 70's, for a square leading edge plate, the sound was shown to feed back on the vortex shedding process causing a step change in the shedding frequency increasing the Strouhal number for the plate by twice the normal value [9].

4.1 Determination of the resonance frequencies of the inclined plate without flow

The acoustic resonance frequencies of the Parker's modes were shown to be real and analytically calculated in the 80's [10] as a function of the ratio L/H between the lengths of the plate located on the centreline of the H high duct. In our experiment, dimensions are such that $L/H = 1$ and the Parker's mode usually called $\beta(0,0)$ with no vertical nodal line can exist. When the plate is off centre in the duct or is inclined, the resonance frequencies [11] becomes complex. A study has also shown that the loss of symmetry of the plate leads to high and sharp Transmission Loss (TL) at these frequencies [12] while it is low and broadband for perfectly symmetric case only depending upon the plate thickness. The resonances frequencies can be detected by measuring the transmission coefficients spectra for several opening flap angles α. In Fig. 5, the measured transmission coefficients for the plane wave mode is compared with a FEM calculation. At 200Hz the experimental transmission coefficient is lower than the numerical one

whatever α because of duct wall vibrations [5]. Results show frequencies below 1717Hz (which corresponds to the cut-off frequency of the second and third transverse duct modes) where the transmission coefficients are sharply decreasing (high TL) depending upon α, except at α = 90° (horizontal position) as expected [12].

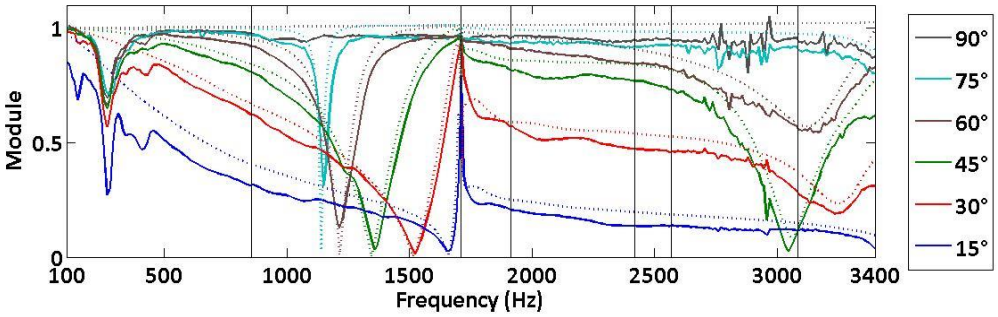

Figure 6: Transmission coefficient from upstream to downstream for plane wave mode without flow. Measured (-) and calculated by FEM (⋯).

A theoretical calculation of the real part of the fundamental resonance frequency (Fig. 8 in [11]) was conducted for an elliptic shape butterfly valve pointing out that the resonance frequencies become complex with a very small imaginary part and decrease when α varies from 0° up to 90° where it becomes real. From a practical point of view, these frequencies can be estimated via Parker's theoretical resonance frequencies which normally hold only for flat plates. It suffices to consider the effective length along the duct axis of the test section occupied by the flap, i.e. $L' = H\sin(\alpha)$. In Table 1, these theoretical resonance frequencies are compared with the experimental ones identified in Fig. 5 (corresponding to sharp dips) showing a very good agreement.

Table 1: Comparison between experimental and theoretical resonance frequencies obtained from [10].

α (°)	f_{th} (Hz)	f_{exp} (Hz)
15	1632	1650
30	1530	1520
45	1360	1350
60	1190	1210
75	1154	1150

A FEM calculation of the acoustic pressure around the flap at α = 75° for an incident plane wave at 1154Hz, closed to the resonance frequency plotted in Fig. 7 shows a pressure distributions in opposite phase on each side of the plate and nodal lines starting from the edges. These pictures shows spatial patterns which are very similar to the β(0,0) Parker's mode.

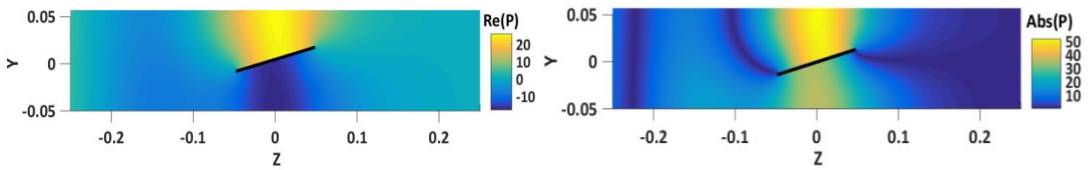

Figure 7: The real part (left) and the modulus (right) of the pressure around the flap (α=75°) corresponding to an incident plane wave at 1154Hz.

Note that the transmission coefficients falls sharply at 3060Hz for the particular case where α=45° and though Parker's theory does not apply here, this illustrates the existence of another acoustic mode around this frequency.

4.2 Analysis of the SWL of the butterfly flap with flow

The SWL of the butterfly flap aero-acoustic source was measured versus flow for several angles α. Results of Fig. 8 for α = 45° shows two maxima around 1500Hz and 3000Hz which emerges from the broadband noise by 20dB. These frequencies seem to coincide with frequencies of Fig. 5.

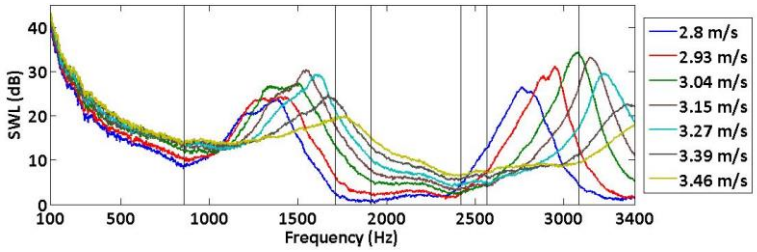

Figure 8: SWL spectra radiated downstream the academic flap for α = 45° and for different flow velocities.

For analysis purpose, a study of the variation of these maxima versus the mean flow velocity was conducted. Physical effect, responsible for the result shown in Fig. 8, has been discussed in previous papers [13] only for horizontal plate. In absence of duct walls, the flow impingement on a horizontal long plate ($L/t = 25$) with square edges allows strong shear layer separation from both the leading and trailing edges and interaction between resultant vortex structures [13]. When the plate is placed centrally in a duct with the long axis parallel to the flow (as shown in Fig. 9), the acoustic mode β(0,0) can be excited if the leading and trailing edge vortex shedding frequency bands overlap the resonance frequency of the duct. From [13], "*If the flow system is receptive to this frequency the flow will become locked and thus complete a feedback loop sustaining the resonance*".

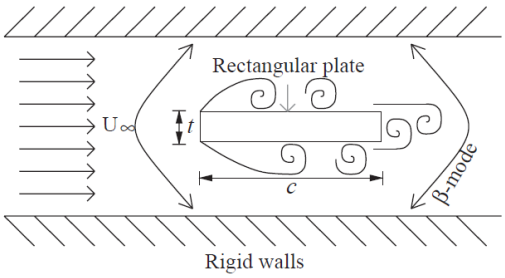

Figure 9: Flow around a square edges plate centred in a duct from [13].

Unlike the flat plate scenario, no research work can be found on inclined flaps with different opening angles. Following the analysis achieved in [9], the level variation of the maximum SWL radiated by the butterfly flap (for the case α = 45°) versus the upstream mean flow velocity U is given in Fig. 10 (each curve corresponds to the two maxima of Fig. 8). It is found that the maximum occurs (see Table 2) respectively at 1500Hz and 3040Hz which is very close to the acoustic resonant frequencies described earlier.

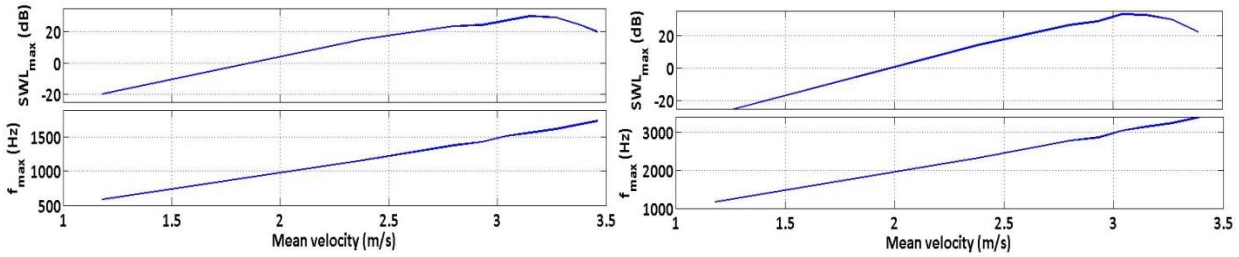

Figure 10: Maximum of SWL radiated downstream the academic flap for the first peak (left) and for the second peak (right) (the opening angle is $\alpha = 45°$).

5. Concluding remarks

Two kinds of feedback effects caused by the interaction of a low Mach number flow with the presence of obstacle(s) inserted in a duct have been experimentally observed. For the case of an inclined flap, it is shown that this feedback mechanism is produced by the coincidence between the plate vortex shedding frequency with a resonant acoustic mode associated with the cavity around the flap. When two diaphragms in tandem are inserted in the duct the feedback is caused by the flow impingement on the second diaphragm placed downstream. This work shows that during the design process of a HVAC system these type of feedback phenomena have to be taken into account to avoid very high level noise amplification. The numerical simulation of such fluid-acoustic resonant effects is also not trivial as the use of classical aeroacoustic analogies based on incompressible-flow solver is not sufficient to simulate correctly these amplifications.

ACKNOWLEDGMENTS

The authors are grateful to the Région Picardie and the FEDER for their financial support.

REFERENCES

1 Nelson, P., Morfey, C. Aerodynamic sound production in low speed flow ducts, *Journal of Sound and Vibration*, **79**, 263–289, (1981).
2 Kreuzinger, J., Schwertfirm, F., Peller, N., Hartmann, M. Analysis of resonance phenomena caused by obstacles in HVAC exhaust nozzles using CFD-CAA approach, AIAA paper 2132, *19th AIAA Aeroacoustics conference*, Berlin, Germany, (2013).
3 Guérin, S., Thomy, E., Wright, M. Aeroacoustics of automotive vents, *Journal of Sound and Vibration*, **285**, 859–875, (2004).
4 Ziada, S. Industrial aeroacoustics: excitation mechanisms and counter-measures, *IV Escola de Primavera de Transição e Turbulência*, (2004).
5 Bennouna et al. Aeroacoustic Prediction Methods of Automotive HVAC Noise, *SAE Noise & Vibration Conference*, Grand Rapids, USA, (2015).
6 Rossiter, J.E. Wind tunnel experiments on the flow over rectangular cavities at subsonic and transonic speeds, Aeronautical Research Council Report and Memorandum N° 3438 (1964).
7 Papaxanthos, N., Perrey-Debain, E., Bennouna, S., Ouedraogo, B., Moreau, S., Ville, J.-M. Pressure-based integral formulations of Lighthill-Curle's analogy for internal aeroacoustics at low Mach numbers, *Journal of Sound and Vibration*, **393**, 176–186, (2017).
8 Parker, R. Resonance effects in wake shedding from parallel plates: calculation of resonant frequencies, *Journal of Sound and Vibration*, **5**(2), 330–343, (1967).
9 Welsh, M.C., Gibson, D.C. Interaction of induced sound with flow past a square leading edge plate in a duct, *Journal of Sound and Vibration*, **67**(4), 501–511, (1979).
10 Koch, W. Resonance acoustic frequencies of flat plate cascades, *Journal of Sound and Vibration*, **88**(2), 233–242, (1983).

11 Duan et al., Complex resonances and trapped modes in ducted domains, *Journal of fluid mechanics*, 571, 119–147, (2007).
12 M Rim and Y Kim. Narrowband noise attenuation characteristics of in-duct acoustic screens. *Journal of Sound and Vibration*, 234(5), 737–759, (2000).
13 Tan et al., Sources of acoustic resonance generated by flow around a long rectangular plate in a duct, *Journal of Fluid and Structures*, **18**, 729–740, (2003).